IEA Wind Task 46

Erosion of wind turbine blades

Pre-evaluation of test specimen

Technical report

Nicolai Frost-Jensen Johansen

James Nash

iea win

Technical Report

Pre-evaluation of test specimen

Prepared for the
International Energy Agency Wind Implementing Agreement

Prepared by
Nicolai Frost-Jensen Johansen, DTU Wind and Energy Systems, DK
James Nash, Ilosta, UK

March 2025

Purpose

Leading edge erosion (LEE) of wind turbine blades has been identified as a major factor in decreased wind turbine blade lifetimes and energy output over time. Accordingly, the International Energy Agency Wind Technology Collaboration Programme (IEA Wind TCP) has created the Task 46 to undertake cooperative research in the key topic of blade erosion. Participants in the task are given in Table 1.

The Task 46 under IEA Wind TCP is designed to improve understanding of the drivers of LEE, the geospatial and temporal variability in erosive events; the impact of LEE on the performance of wind plants and the cost/benefit of proposed mitigation strategies. Furthermore Task 46 seeks to increase the knowledge about erosion mechanics and the material properties at different scales, which drive the observable erosion resistance. Finally, the Task aims to identify the laboratory test setups which reproduce faithfully the failure modes observed in the field in the different protective solutions.

This report is a product of Work Package 4 Laboratory testing of erosion.

The objectives of the work summarized in this report are to:

- Assess the effectiveness of RET inline imaging for detecting and classifying pre-existing defects in coating materials.
- Investigate the impact of pre-existing defects on incubation detection and their influence on VN curves and lifetime predictions.
- Quantify the limitations of inline RET inspections, including challenges such as motion blur, SNR trade-offs, and perspective distortion.
- Address the need for different levels of inspection (Levels 1-4) to determine when higher-resolution or external imaging methods may be necessary.
- Propose possible improvements to RET imaging, including lighting enhancements (high-intensity strobes) and alternative inspection techniques.
- Establish guidelines for defect classification and baseline imaging, ensuring consistency in rain erosion testing and material evaluation.

Table 1 IEA Wind Task 46 Participants.

Country	Contracting Party	Active Organizations
Belgium	The Federal Public Service of Economy, SMEs, Self-Employed and Energy	Engie
Canada	Natural Resources Canada	WEICan
Denmark	Danish Energy Agency	DTU (OA), Hempel, Ørsted A/S, PowerCurve, Siemens Gamesa Renewable Energy
Finland	Business Finland	VTT
Germany	Federal Ministry for Economic Affairs and Energy	Fraunhofer IWES, Covestro, Emil Frei (Freilacke), Nordex Energy SE, RWE, DNV, Mankiewicz, Henkel
Ireland	Sustainable Energy Authority of Ireland	South East Technology University, University of Galway, University of Limerick
Japan	New Energy and Industrial Technology Development Organization	AIST, Asahi Rubber Inc., Osaka University, Tokyo Gas Co.
Netherlands	Netherlands Enterprise Agency	TU Delft, TNO
Norway	Norwegian Water Resources and Energy Directorate	Equinor, University of Bergen, Statkraft
Spain	CIEMAT	CENER, Aerox, CEU Cardenal Herrera University, Nordex Energy Spain
United Kingdom	Offshore Renewable Energy Catapult	ORE Catapult, University of Bristol, Lancaster University, Imperial College London, Ilosta, Vestas
United States	U. S. Department of Energy	Cornell University, Sandia National Laboratories, 3M

Table of Contents

List of Figures

List of Tables

Executive Summary

This report evaluates the effectiveness of inline imaging in Rain Erosion Testing (RET) for detecting and classifying pre-existing defects in coating materials. While inline imaging provides the largest dataset for analysis, limitations such as motion blur, SNR trade-offs, and perspective distortion can impact defect detection accuracy.

The study investigates how pre-existing defects influence incubation detection and VN curves, particularly in cases where features like pinholes appear early but do not indicate true material loss. This can lead to misinterpretation of coating performance and lifetime predictions.

To improve RET imaging, the report explores potential lighting enhancements (high-intensity strobes) and better calibration methods to reduce distortion. Standardizing defect classification guidelines is also essential to ensure consistent and reliable evaluation.

While inline RET imaging is valuable for baseline inspection, alternative methods may be necessary in cases where defect detection accuracy is critical. The findings provide a foundation for optimizing RET protocols to enhance test reliability and material evaluation.

1. Pre-damage Evaluation and Defect Detection for Coating Failure Assessment and Incubation Analysis

As specified in Deliverable 4.2 [3], detecting incubation is the primary goal of rain erosion testing (RET). RET serves two main roles:

1. Lifetime prediction and coating certification – RET is a key tool for evaluating coating durability as part of lifetime estimation models, as referenced in [1].
2. Material development and verification – RET is used by coating developers to assess material improvements and performance under erosive conditions.

In both cases, damage detection and evaluation are essential. For lifetime estimation, defects may be unavoidable, and the argument is that if a 430 mm RET specimen cannot be manufactured without defects, then neither can the 10-30 meter-long critical leading edge protection (LEP). This necessitates an understanding of how defects influence incubation and propagation.

For material development, defects may arise as an unintended side effect in early coating formulations. However, the primary focus at this stage is on the intrinsic incubation performance of the base material rather than on minor defects. Therefore, it is important to identify and separate defect-induced damage from genuine material incubation performance.

There is a clear need to determine how defects can be detected—both during and prior to RET—and to establish the level of detection required for effective analysis.

2. Levels of Inspection for RET Specimens

The structure for the report will focus on different levels of inspection that can be employed for RET specimens shown in Figure 1.

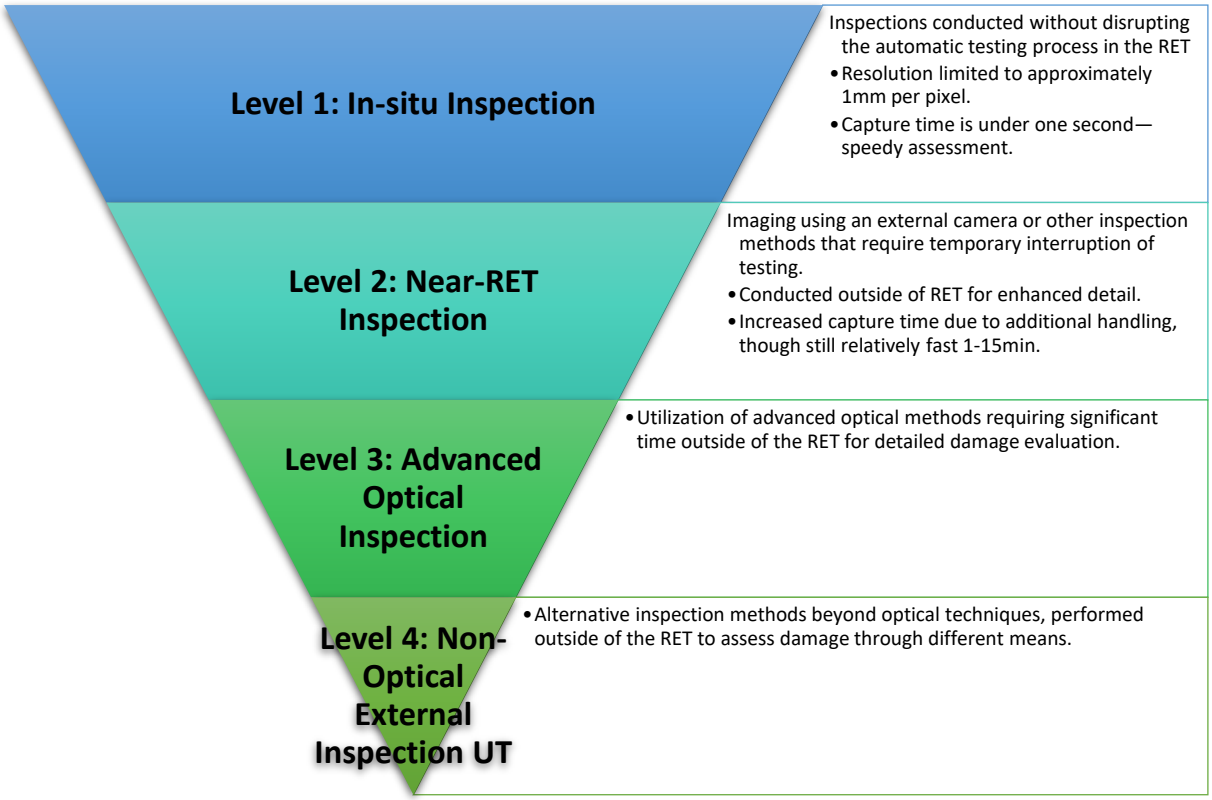

Figure 1. Different levels of inspection for rain erosion test specimen.

- **Level 1: In-situ Inspection** - Inspections conducted without disrupting the automatic testing process in the RET.
- **Level 2: Near-RET Inspection** - Imaging using an external camera or other inspection methods that require temporary interruption of testing.
- **Level 3: Advanced Optical Inspection** - Utilization of advanced optical methods requiring significant time outside of the RET for detailed damage evaluation.
- **Level 4: Non-Optical External Inspection UT** - Alternative inspection methods beyond optical techniques, performed outside of the RET to assess damage through different means.

For this report we will focus on the use of the inline system **Level 1: In-situ Inspection, Level 2: Near-RET Inspection and Level 4: Non-Optical External Inspection UT** to understand and extract the maximum amount of information, on what is the baseline capture for all RET tests

3. Level 1: In-situ Inspection

This refers to inspections that can be conducted without disrupting the automatic testing process in the RET.

The modern generation of RETs that conform to DNV [1][2] primarily rely on an inline camera system to image the specimen during testing. Imaging is not performed entirely in situ but rather at set intervals, down to a minimum of one minute. After each interval, the rain field is turned off, and the rotor undergoes a drying phase. Once dried, the rotor is decelerated to the imaging speed of 5 rpm.

During imaging, each blade is illuminated along its length, and a picture is captured when the blade is positioned normal to the camera's line of sight. This method ensures consistent imaging conditions while maintaining an automated testing process. The camera is placed approximately 2.5 meters away from the sample and zoomed in to cover the visible span of 430 mm.

A benefit of the camera position is that it minimizes perspective distortion. At this distance, the half-angle deviation from telecentricity is approximately **5°:**

$$\theta = \tan^{-1}\left(\frac{0.43m/2}{2.5m}\right) = 5°$$

which means the system is relatively close to telecentric but not perfectly so. This results in reduced but still present perspective effects, ensuring that measurements across the span remain fairly accurate without significant scaling distortions.

In comparison, if the camera were placed at **arm's length** (~0.7 m away), the half-angle deviation would increase significantly. Using the same calculation:

$$\theta = \tan^{-1}\left(\frac{0.43m/2}{0.7m}\right) = 17°$$

This would result in a deviation of approximately **17°**, meaning perspective distortion would be much more pronounced. Objects closer to the camera would appear disproportionately larger than those farther away, making it harder to achieve accurate and consistent measurements.

Thus, placing the camera farther from the sample reduces these distortions and improves the reliability of imaging for erosion analysis. However, for applications requiring even greater accuracy, a **telecentric lens** would be necessary to eliminate perspective effects entirely.

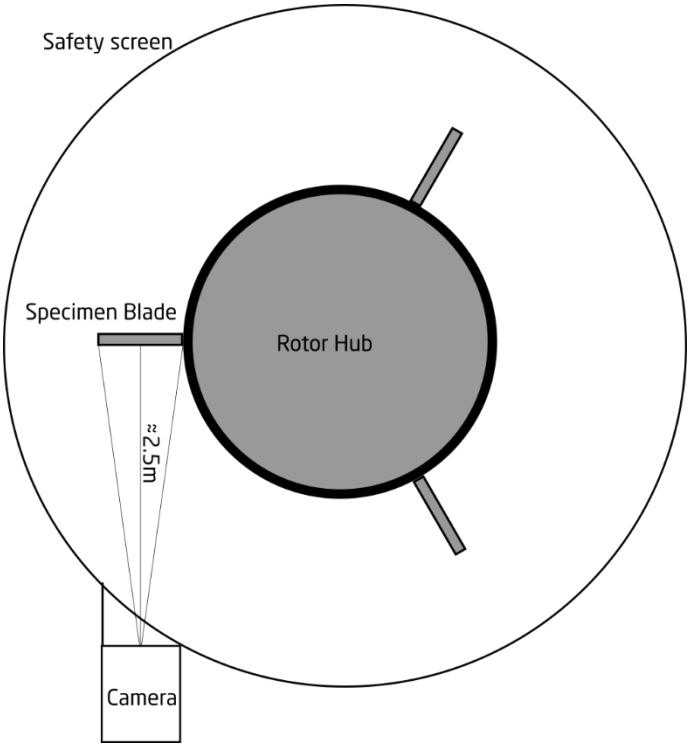

Figure 2 Illustration to approximate scale of the average R&D A/S RET, with camera position shown and approximate distance from camera to specimen at imaging position.

As a result of the RET imaging system, the sample will always be moving during image capture at an angular velocity of **0.5 rad/s**, with a **closing velocity of 0.6 m/s** at the blade tip. Therefore, the camera's shutter time must be short to minimize motion blur and ensure clear image acquisition.Figure 2 shows the geometry.

To estimate the worst-case blur, we consider a point at the **tip of the blade**, where motion in the spanwise direction is most pronounced as the blade moves toward the camera. This relationship between shutter speed and motion blur is visualized in **Figure 3**.

Since we are looking for **incubation damage of approximately 1 mm in size** [3], we apply a general rule of thumb: motion blur should be less than **50% of the feature size** to ensure clear detection. From the plot, we can determine that to keep the blur below **0.5 mm**, the shutter speed must be **less than 900 µs**.

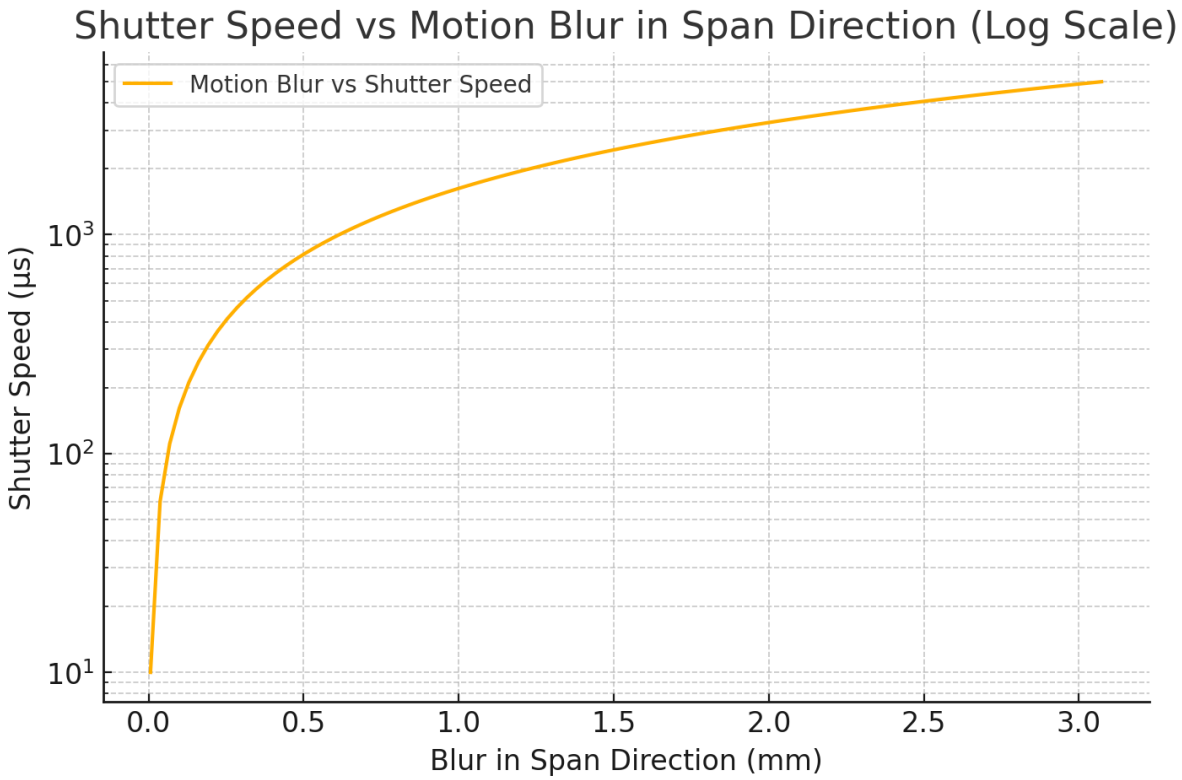

Figure 3 Relationship Between Shutter Speed and Motion Blur.

However, we cannot have infinitely short exposure times. To maintain the same exposure level, we must increase the **gain/ISO** of the sensor, which leads to increased image noise.

With the current state-of-the-art global shutter 16MPX camera used in the RET, we obtain an SNR of approximately 40 at 1000 microseconds of exposure. There are general guidelines for SNR in analytical work:

- **Yellow (30-50 SNR):** Acceptable – Some noise, but usable.
- **Orange (50-100 SNR):** Good – Suitable for quantitative analysis.
- **Green (100-200 SNR):** Very Good – Reliable for high-precision work.
- **Blue (>200 SNR):** Excellent – Ideal for minimal noise applications.

The relationship between SNR and shutter speed can be calculated, as shown in Figure 4. The measured SNR of 40 at 1000 µs serves as a reference to estimate the possible SNR at different shutter speeds.

From the plot, we see that the RET imaging system falls just within the acceptable range. However, this also highlights the limitations of the current state-of-the-art RET imaging system, particularly in applications requiring higher precision and lower noise.

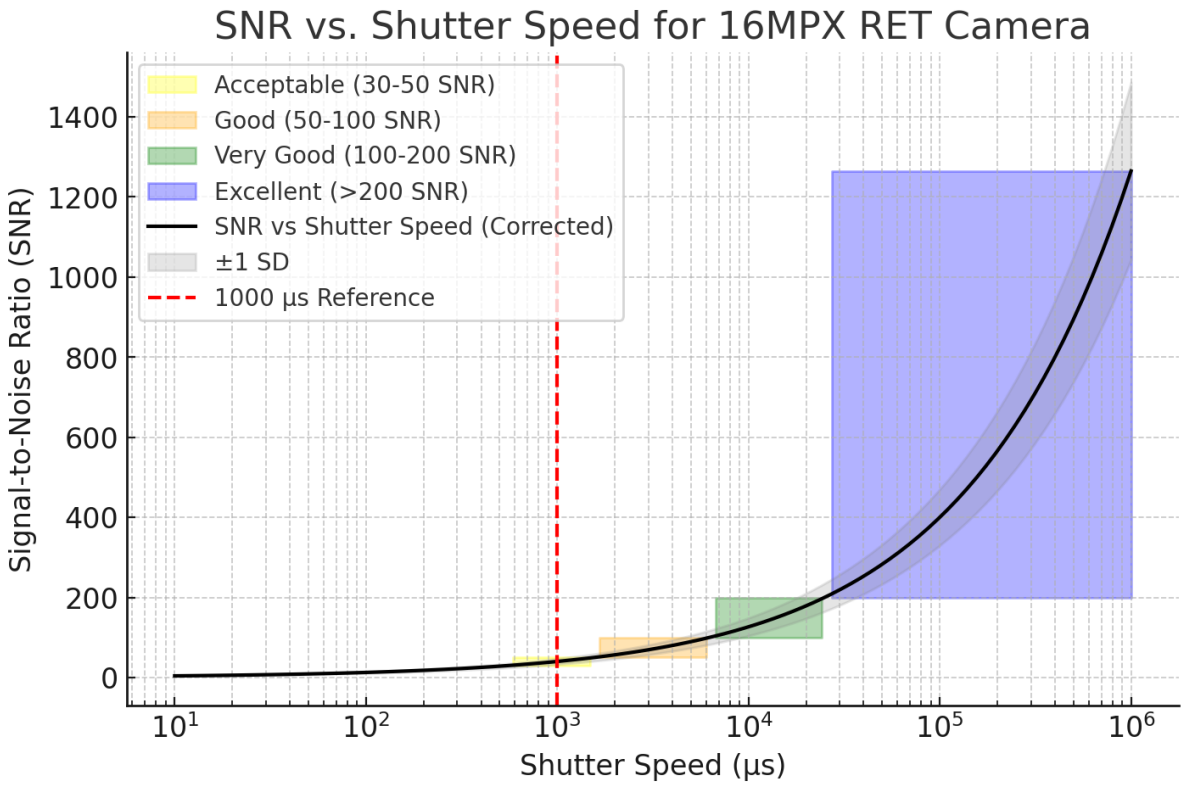

Figure 4 SNR vs. shutter speed for the 16MPX RET camera, showing how signal-to-noise ratio decreases as exposure time is reduced. The shaded regions indicate different quality levels for analytical work, with a red dashed line at 1000 µs marking the reference SNR of 40.

So we can combine the two plots to see the consequences on image quality, as shown in Figure 5. This visualization highlights the trade-offs between motion blur and signal-to-noise ratio (SNR) as a function of shutter speed.

As exposure time decreases, motion blur is reduced, improving the sharpness of the image. However, this comes at the cost of increased noise, as shorter exposure times require a higher gain or ISO setting to maintain brightness. The plot helps illustrate this balance by displaying motion blur on one axis and SNR on the other, both plotted against shutter speed.

From the data, it is evident that at very short shutter speeds, blur becomes negligible, but noise increases significantly. On the other hand, longer shutter speeds improve SNR but introduce motion blur, which can obscure fine details. The reference point at 1000 microseconds, where an SNR of 40 was measured, falls within an acceptable range for analytical work but highlights the limitations of the current imaging system in capturing both sharp and low-noise images simultaneously.

This trade-off is crucial when selecting optimal imaging settings for rain erosion testing, where both fine detail resolution and sufficient signal quality are necessary for accurate defect detection and incubation analysis.

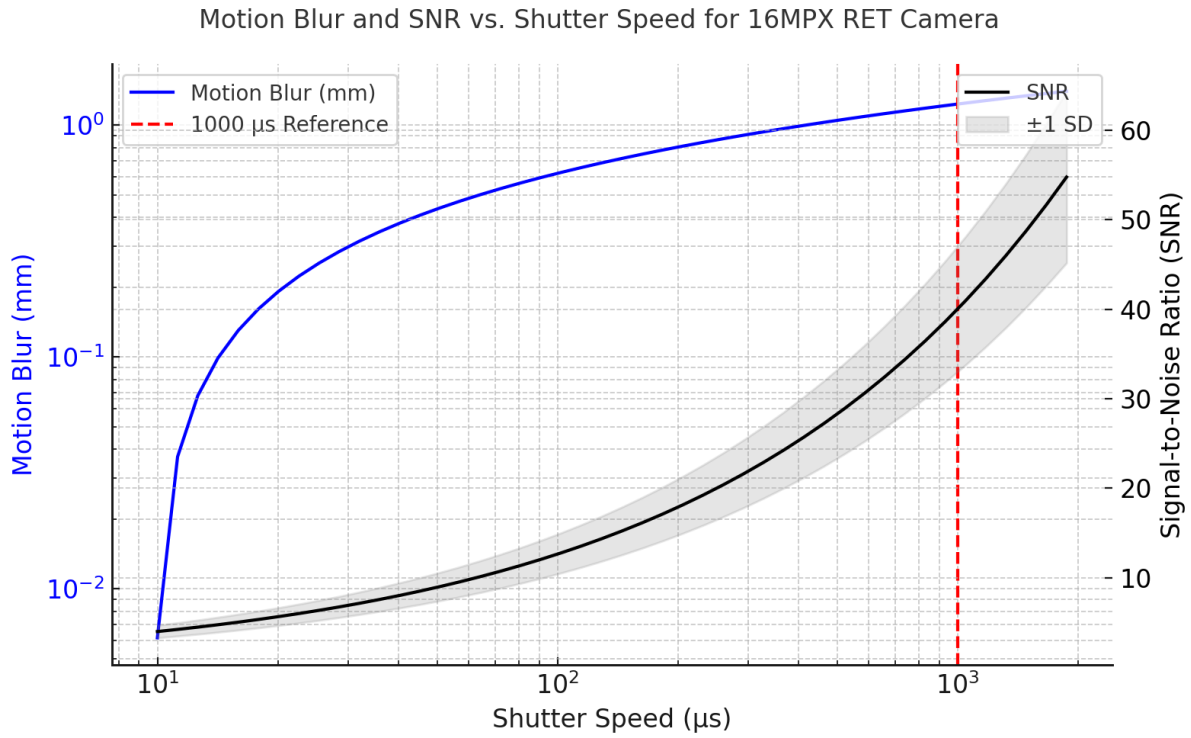

Figure 5 Motion Blur and SNR vs. Shutter Speed for the 16MPX RET Camera.

3.1 Quality of camera used in RET

Over time, the quality of the camera system used in the Rain Erosion Tester (RET) has improved significantly. The original machines from around 2015 were equipped with 1.5 MPX sensors, whereas the current RET systems in 2024 now use 16 MPX sensors. This increase in resolution allows for finer detail capture, improving the ability to detect small incubation damage and erosion patterns.

However, as sensor resolution increases while all other factors remain the same, the signal-to-noise ratio (SNR) decreases, as shown in Figure 6. This happens because higher resolution sensors have smaller individual pixels, leading to less light collected per pixel. Since the total light captured by the sensor remains constant, the per-pixel signal decreases, while the noise, primarily photon shot noise and read noise, does not scale down proportionally.

This means that while higher resolutions allow for smaller feature detection, they also introduce more noise, which can reduce the effective gain in detail resolution. If the pixel size becomes too small, the signal may become dominated by noise, making it difficult to distinguish fine incubation features from random fluctuations in brightness.

With by placing a video camera in a similar position to the inline camers we illustrate the effect of the blur on sharpness

Figure 6. The left is shown a still from video taken while RET is at capture speed 5rpm. To the right is shown the same blade at testing speed 160m/s.

At some point, simply increasing resolution does not provide a practical benefit unless other parameters such as exposure time, sensor sensitivity, or noise reduction techniques are improved. This trade-off is crucial when optimizing the RET imaging system for erosion damage detection, ensuring a balance between high spatial resolution and sufficient image clarity for accurate analysis.

If the illumination of the samples is not increased accordingly, Figure 7 shows that further resolution gains may not significantly improve image quality due to the limitations imposed by SNR. In such cases, the system reaches a point where additional pixels do not provide better detail but instead amplify noise, making it necessary to adjust other imaging parameters to fully utilize the benefits of higher-resolution sensors.

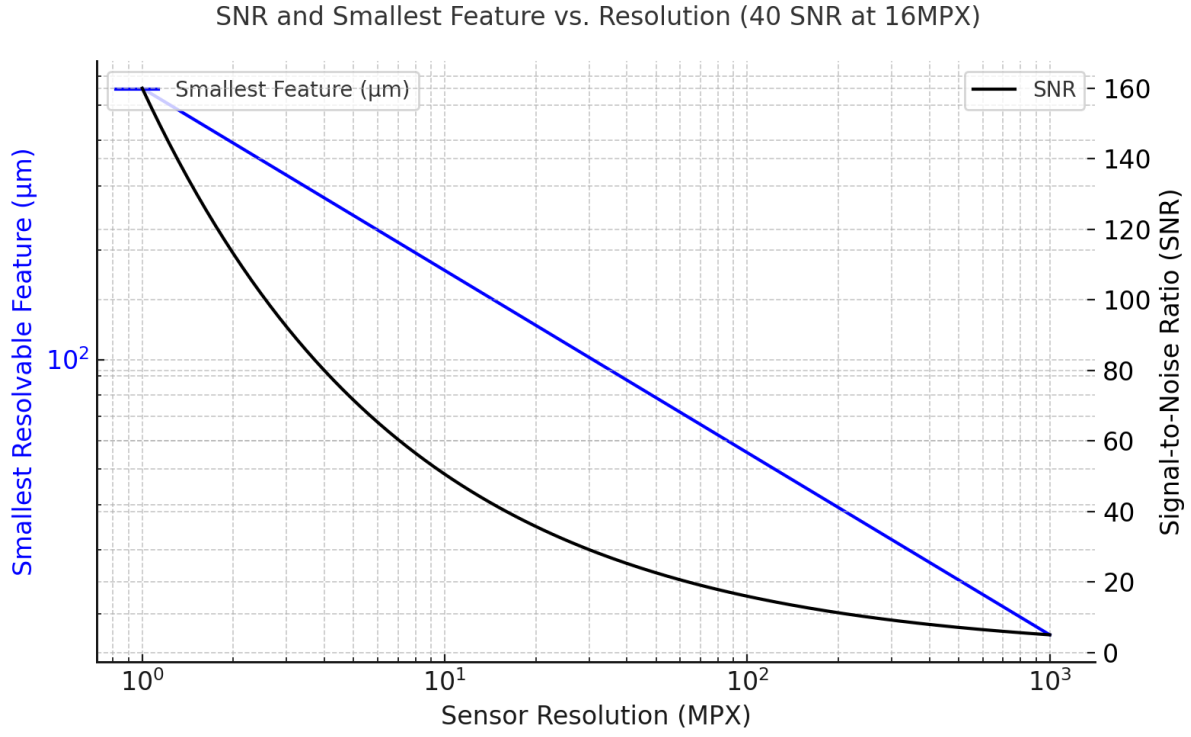

Figure 7 Effect of Increasing Sensor Resolution on SNR.

The ideal solution to the imaging problem would be to upgrade the lighting system to a high-intensity strobe. This would allow for freezing motion while providing proper illumination of the sample. Historically, this approach was used in some of the original RET systems from the 1970s, where analog video cameras and xenon strobes were employed to capture motion-free images.

4. Level 2: Near-RET Inspection

One option to achieve better image quality is to capture images of the sample while it is stationary. This is typically done by removing the blade from the RET and mounting it in a dedicated photo rig. This setup allows for longer exposure times, negating the trade-off in signal-to-noise ratio (SNR) that we face when imaging in the RET.

An example of this type of image can be seen in Figure 8. Here, the exposure is optimized. However, one challenge with this approach is the increased perspective distortion due to the short distance between the camera and the sample. If not corrected, this distortion can lead to measurement inaccuracies

Typically, we use a two-point calibration based on the longest distance in the image, which in this case is 440 mm. When measuring from one side, a small but noticeable cumulative error in radial position arises between the edge of the sample and the optical center. This is evident in the image, where based on pixel distance calibration, we assume a measurement of 100 mm, but when checked against a scale, the actual measurement is only 99 mm. While small, this systematic error affects velocity measurements on the sample.

In principle, this error can be corrected using a geometric transformation, but in practice, it is rarely done. As a guideline for sample imaging outdoors, it is recommended to maximize the distance between the camera and the sample to minimize perspective distortion.

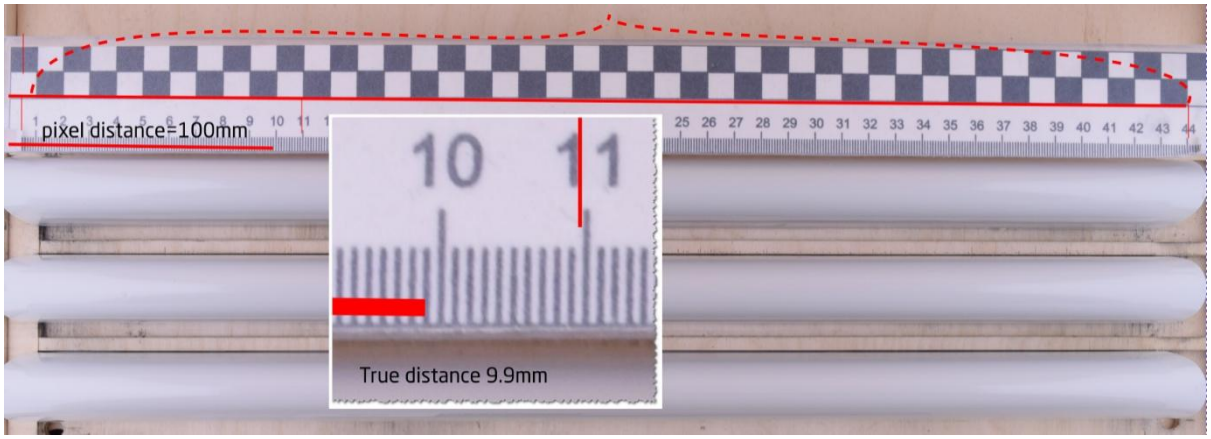

Figure 8 Example images of a RET samples photographed outside of the RET.

As a worst-case example of the distortion that can occur on a **435 mm-wide sample positioned 700 mm away** from the camera, we observe a distinct distortion profile, as shown in **Figure 9**. In this scenario, perspective effects cause a cumulative positional error, where points further from the optical center appear shifted due to the nonlinear mapping of real-world distances onto the image plane. The distortion is minimal at the **center** and **edges** of the field of view but peaks at intermediate positions, forming a characteristic **M-shaped error profile**. This effect can lead to small but systematic measurement inaccuracies, particularly when relying on direct pixel-based distance calibrations without correction for perspective distortion.

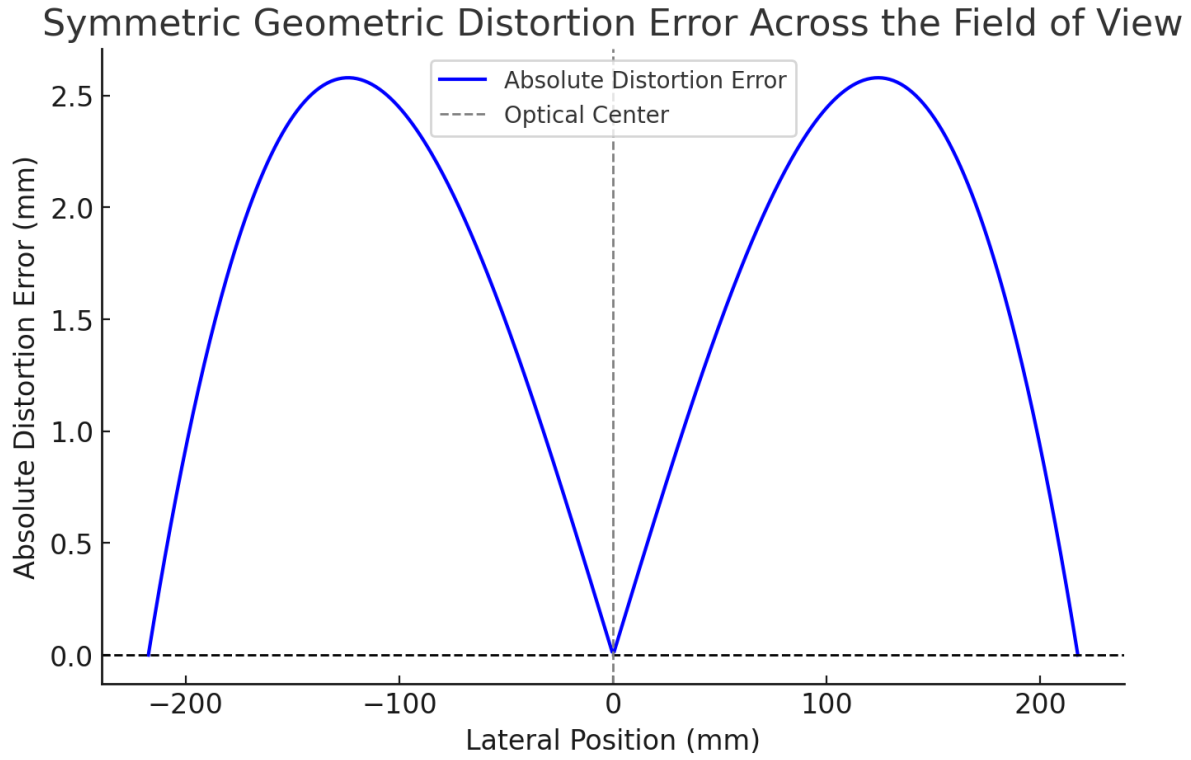

Figure 9 M-shaped absolute error in measured distance relative to the optical center, with known positions at both ends of the sample.

4.1 Example of defects observable in RET inline camera - pinholes

Several types of pre-existing defects can still be observed despite the limitations of the RET imaging system. Among them, pinholes are the most common, as illustrated in Figure 10. These defects typically form when small pre-existing bubbles in the coating become capped off during early inspections. Over time, these areas appear as dark spots, likely due to small amounts of eroded material collecting in the pits and absorbing light, enhancing their contrast in the image.

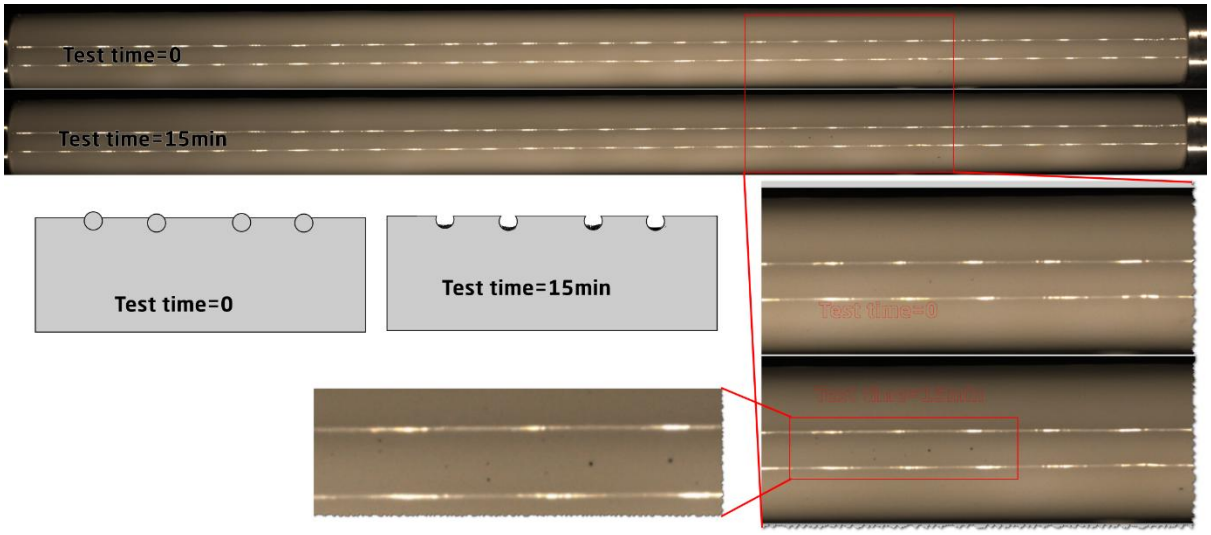

Figure 10 shows how pinholes get exposed early on in the erosion process.

This effect is reflected in the area growth rate of damages on blades with pinholes, where many damages are distributed across a wide velocity range, as shown in Figure 11. However, we also observe that while some damages show little to no evolution in area as a function of impingement, others grow rapidly. A possible hypothesis is that at high speeds, a pinhole can act as an initiating or accelerating factor, leading to early damage once the material surpasses its damage threshold, as observed by Evans [3].

This provides additional insight into materials and tests where the presence of pre-existing defects can significantly impact the validity of VN curves. The appearance of pinholes does not truly represent the incubation phase, as there is no significant loss of coating immediately after their first visual detection. As a result, the VN curves can become unreliable, as illustrated in Figure 12.

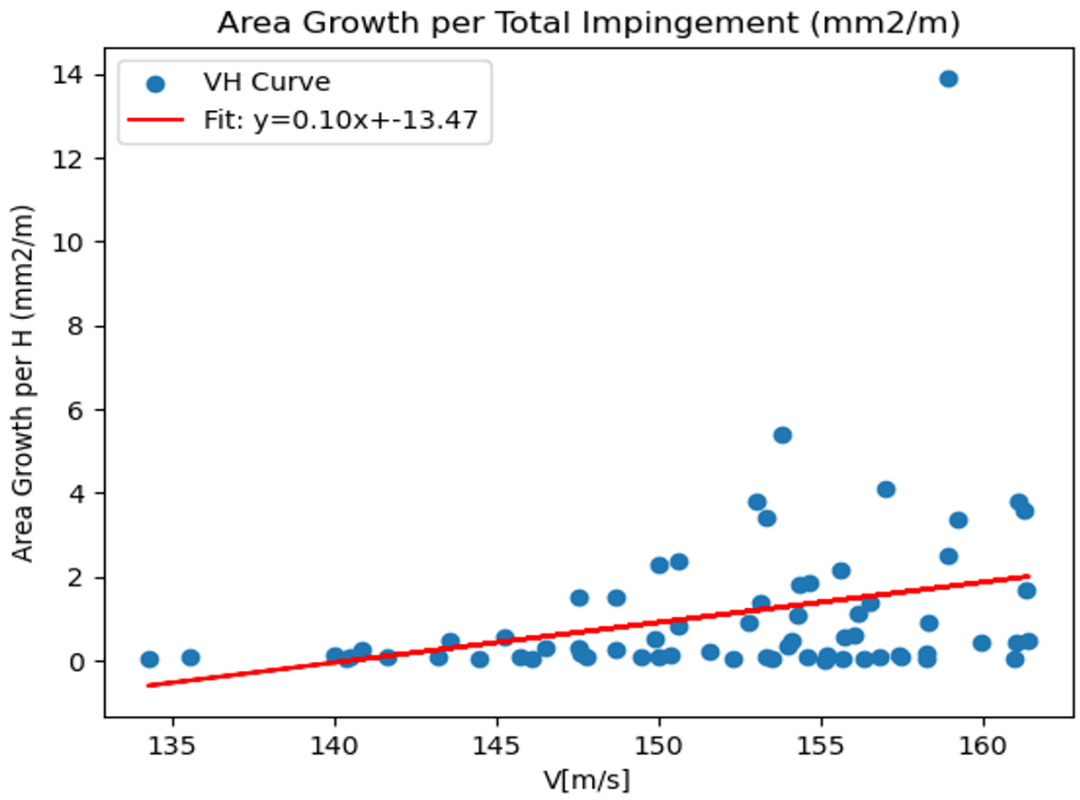

Figure 11 Shows the area growth rate as measured using DTU-RETINA annotation tool.

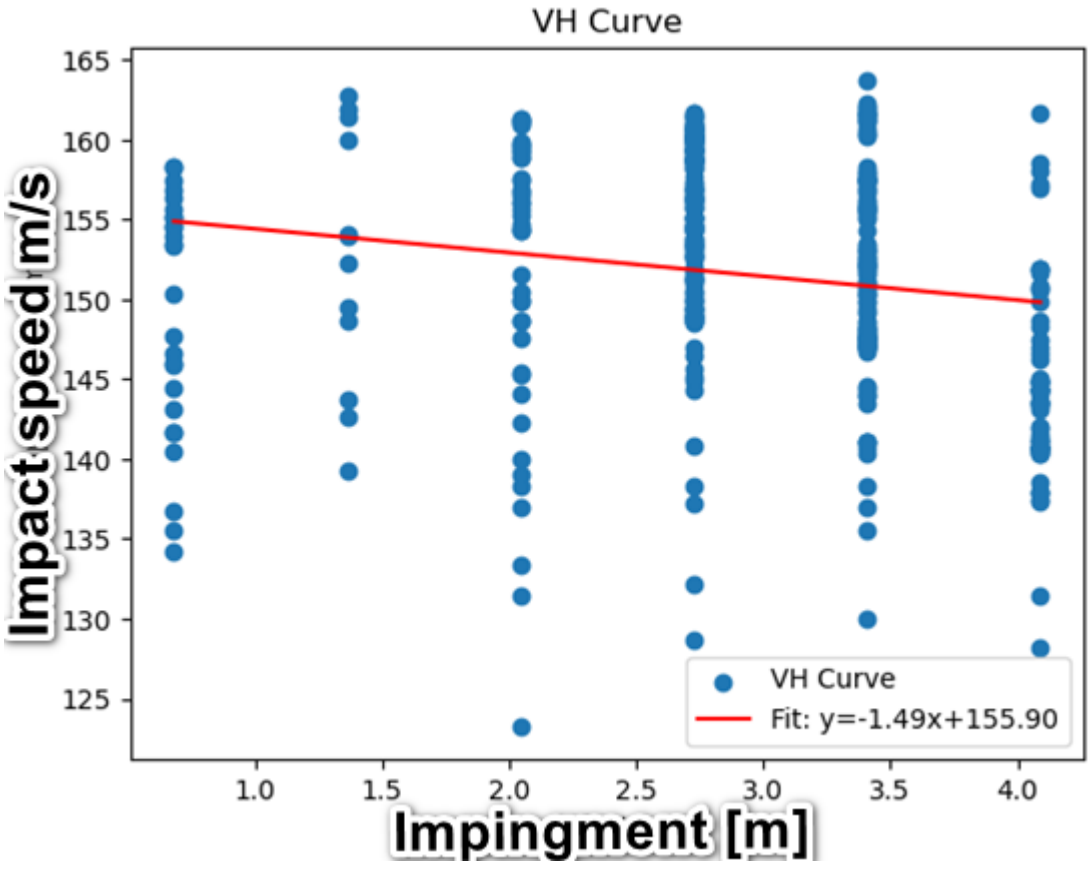

Figure 12 Shows the VH curve for a material presenting with many pinholes.

4.2 Lighting Limitations and Resolution Constraints

The current **16 MPX inline camera** offers a balance between resolution and sensitivity, but further improvements may be needed, such as high-intensity strobes to freeze motion and improve image clarity.

If these **limitations cannot be fully addressed**, it may be necessary to move to **higher levels of inspection** (Level 2, 3, or 4) for a **comprehensive understanding** of how **pre-existing defects** affect **RET performance across different coating materials**. This may include:

- **Near-RET Inspection (Level 2):** Using **external cameras** for improved resolution and control over imaging conditions.
- **Advanced Optical Inspection (Level 3):** High-magnification imaging and **structured light scanning** for precise damage measurement.
- **Non-Optical External Inspection (Level 4):** Alternative inspection techniques such as **X-ray CT scanning** or **ultrasound analysis** for subsurface defect characterization.

Ultimately, while RET inline imaging provides the largest and most accessible dataset, certain cases—especially involving pre-existing defects—may require more advanced inspection techniques to fully understand their impact on coating incubation and erosion performance.

5. Level 4: Non-Optical External Inspection: Alternative inspection techniques such as X-ray CT scanning or ultrasound analysis for subsurface defect characterization.

Ultrasound presents an opportunity to investigate surface and sub surface defects on leading edge protection systems. The practical process for investigating the presence of defects, would involve the demounting of test samples from the RET and would likely require the use of a water coupling medium, thus requiring the sample to be submerged inside a tank during inspection. The sample may then require some drying post inspection before mounting the sample back in place. Care must be taken to ensure that the composites, fillers, adhesives and other materials present in the test coupon are suitable to be submerged in water for extended periods of time. In practice, unlike other NDT methods, a full-sized RET sample could be used for testing and inspection, however most systems are not designed for the inspection of curved samples and so some additional setup and processing would be required to build a system for inspection.

During ultrasound, acoustic waves are emitted from a transmission source, which penetrates a material. When there is a difference in acoustic properties, a portion of the wave energy is reflected back in the original direction of travel and is received by a data acquisition system. This is typically how defects are detected.

The smallest resolvable feature during an ultrasound inspection is dependent on the spatial sampling resolution (x-y), the sampling frequency of the data acquisition system (depth resolution), the frequency of the ultrasound probe and the acoustic

velocity of the material. In general, the most common ultrasound probes use compressive waves from which the acoustic velocity, v relates to the young's modulus, E, and density, ρ, of the material via the equation:

$$v = \sqrt{\frac{E}{\rho}}$$

The acoustic velocity of the material then relates to the frequency, f, of the selected probe and its respective wavelength, λ, using the following equation:

$$\lambda = \frac{v}{f}$$

This is important as the minimum resolvable size that something with a differing acoustic impedance can be detected is approximately 0.5 times the wavelength of the selected inspection frequency (as illustrated in Figure 14). However, surface topology and sample thicknesses can be determined directly, to inspect irregularities or areas of reduced coating thickness (As illustrated in Figure 13).

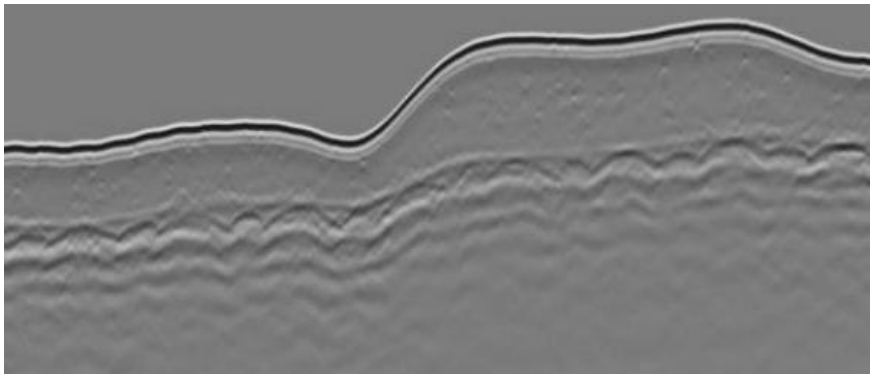

Figure 13: Surface topology of a coated composite sample using a scanning acoustic microscope. The black line in the image represents the surface of the coating, with the wavey surfaces below showing the composite layers. Defects within the coating barely are visible in this image.

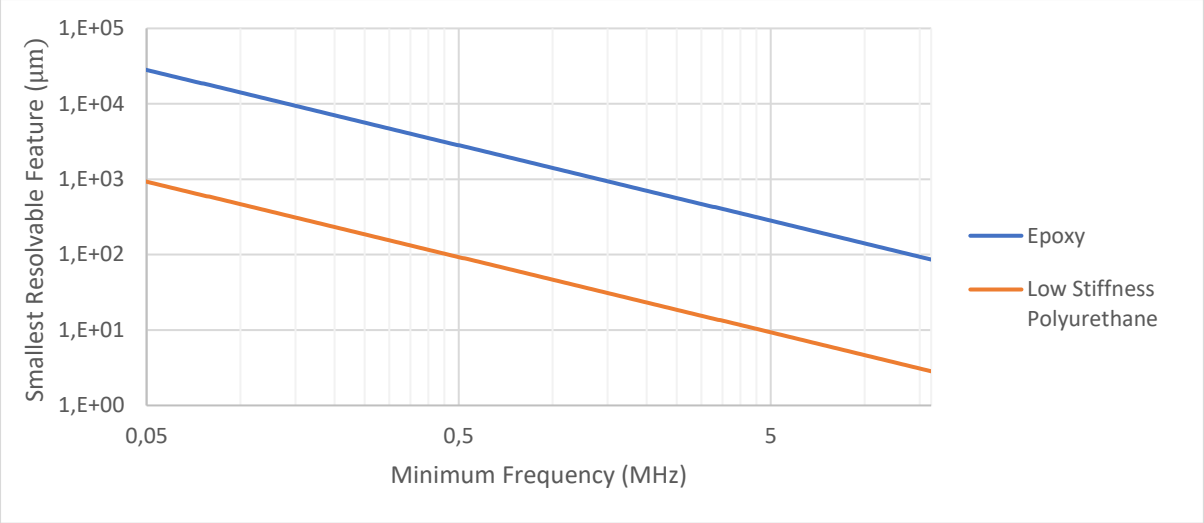

Figure 14: Minimum resolvable size feature for a low stiffness polyurethane vs an epoxy.

The other factor to consider is the difference in acoustic impedance between the parent material and the material trying to be detected which is given by:

$$Z = \rho v$$

The combined effect of acoustic impedance mismatch, defect geometry and internal sample geometry determine the signal strength received for a given defect. For air bubbles, voids or delamination, there is a significant acoustic impedance difference, making detection easier then, for example, the interface between two similar polymers. So, in practice this means that extracting features between two objects with similar material properties may be complicated to do whilst also ensuring that feature can be extracted from the signal noise. This also presents challenges when trying to detect smaller voids in composites that are comparable to the fibre size in composites (As illustrated in Figure 15). However, it is possible to investigate that coatings that protect composites and the interfaces between these coatings and composites.

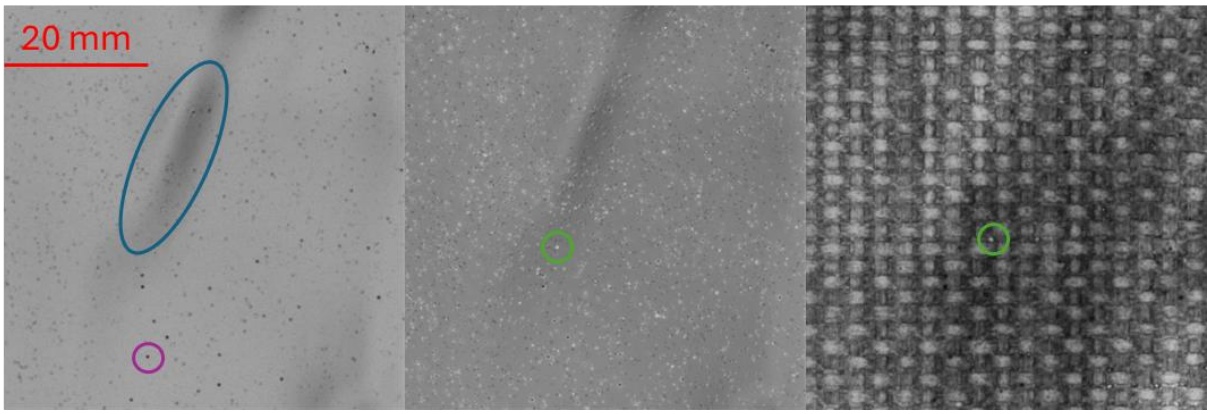

Figure 15: Example ultrasound inspection of a coating surface, subsurface and coating-composite interface. Voids are visible (circled in green), pinholes are visible in purple and surface waviness are visible in blue.

If a multi-layer system is being investigated such as an LEP with a filler or a composite sandwich panel then further considerations must be made as to how the acoustic wave will pass through a secondary material and how it will interact with

features in that second material. For example, if the material has a crystalline structure that has grains large enough to interact with the acoustic waves or for example if the material has a fibrous structure. For multilayer LEPs, if there is a desire to detect voids within the filler portion of the LEP, then these considerations must be made. The interfaces between different layers inside an LEP produce reflections, which can then become visible in later portions of the signal, which can make feature extraction more complex and so being able to interpret and understand ultrasound signals can require some skill.

Defect tolerance within LEPs is currently unknown and the interaction between defects and leading-edge erosion requires further work, so defining an inspection program is not currently possible. However, it can be assumed that defect sizes close to the coating layer thickness are particularly hazardous to LEPS and so defects of interest would be of the order of 100-500 microns [5].

6. Conclusion

In conclusion, it is possible to use the lowest level of inspection in the RET system to detect and classify pre-existing damage. As this method serves as the baseline inspection for all specimens, it also represents the largest available dataset for analysis. However, as outlined in this report, there are several potential pitfalls and shortcomings associated with relying solely on inline RET imaging for defect detection and incubation assessment.

Challenges and Limitations of RET Inline Inspection:

1. Perspective Distortion: a. While minimized due to the camera’s placement, residual perspective distortion can lead to small but systematic measurement errors, particularly in radial position calibration. This is especially relevant for fine incubation damage detection.

2. Motion Blur vs. Signal-to-Noise Ratio (SNR) Trade-off: a. The imaging system must balance motion blur and SNR by adjusting exposure time. A shorter exposure minimizes blur but introduces noise, while a longer exposure improves SNR but increases blur. This trade-off places a fundamental limit on image quality.

3. Defect Misclassification: a. Pre-existing defects such as pinholes can be detected in the inline RET system, but their impact on incubation and erosion progression is difficult to quantify. b. Pinholes may create misleading incubation curves, where damage appears early but without true material loss. This can lead to inaccurate VN curves, requiring additional validation.

4. Non-Optical External Inspection (Level 4): a. Alternative inspection techniques such as X-ray CT scanning or ultrasound analysis can be employed for

subsurface defect characterization. b. Ultrasound allows for surface and subsurface defect detection in leading edge protection systems, but requires careful handling of test samples, including demounting, submersion in a coupling medium, and post-inspection drying. c. Acoustic impedance differences between materials impact defect visibility, making voids, delaminations, and interfaces between dissimilar materials easier to detect than subtle variations within similar polymers. d. The complexity of interpreting ultrasound signals increases with multilayer LEPs, requiring expertise in analyzing reflections and signal noise. e. Current defect tolerance levels within LEPs are not well established, but defects on the order of 100-500 microns are likely to be critical, warranting further study.

By integrating Level 4 inspection techniques, it is possible to enhance defect detection capabilities beyond what inline RET imaging alone can achieve. However, implementing such methods requires careful consideration of material compatibility, test setup feasibility, and data interpretation challenges.

7. References

[1] DNV-GL. (2020). DNVGL-RP-0573: Evaluation of erosion and delamination for leading edge protection systems of rotor blades. December 2020.

[2] DNV-GL. (2018). Recommended practice — DNVGL-RP-0171 (Issue February 2018).

[3] WP4.2 Johansen, N. F.-J. (2023) Erosion failure modes in leading-edge systems. IEA-Wind_Task46_WP4.2-Erosion-failure-modes-in-leading-edge-systems

[4] Evans, A. G., Ito, Y.M., Rosenblatt, M. (1980). Impact damage thresholds in brittle materials impacted by water drops. *Journal of Applied Physics*, 51. https://doi.org/10.1063/1.32802 1

[5] J. Chen and S. J. Bull. Approaches to investigate delamination and interfacial toughness in coated systems: an overview. Journal of Physics D: Applied Physics, 44(3):034001, 2010